Preparation and Interaction Characteristics of Organically Modified Montmorillonite Nanocomposite with Miscible Polymer Blend of Poly(Ethylene Oxide) and Poly(Methyl Methacrylate)

S. K. Lim, J. W. Kim, I. Chin, Y. K. Kwon, and H. J. Choi*

Department of Polymer Science and Engineering, Inha University, Incheon 402-751, Korea

Received May 21, 2001. Revised Manuscript Received February 12, 2002

The intercalation of organically modified montmorillonite (OMMT) in the polymer blend of poly(ethylene oxide) (PEO) and poly(methyl methacrylate) (PMMA) has been demonstrated using dichloromethane as the cosolvent at room temperature. X-ray diffraction has been used to confirm the formation of nanoscale polymers-OMMT hybrids and the localization of the polymers between the organosilicate layers. The silicate nanocomposites have higher tensile modulus and elongation at break than the polymer matrix, revealing the dispersion of the clay particles in the polymer matrix. The specific interaction between the components was quantified by the Flory−Huggins interaction parameters, *B*, for pairs, determined by combining the melting point depression and the binary interaction model. The estimated *B* values for the binary PMMA/OMMT and PEO/OMMT pairs were all negative, showing both proper intercalation of the polymer into the gallery of OMMT and the homogeneous dispersion of OMMT in the polymer matrix. The *B* value for the PMMA/OMMT pair was smaller than that measured for the PEO/OMMT pair, suggesting that PMMA had better affinity for OMMT than PEO.

Introduction

Recently, polymer matrix nanocomposites with organically modified layered silicates have received much attention,[1−3] due to their enhanced mechanical and barrier properties and high temperature stability, as compared with their microcomposite and macrocomposite counterparts. The dispersion of a few percent of layered silicates in the polymer matrix has been carried out by impregnation and direct adsorption. High aspect ratio flakes or platelets have been previously used to improve strength of the polymer matrix as reinforcement materials[4] and gas barrier properties of low and medium barrier polymers. Due to the small enthalpy of mixing of polymer and layered silicates, the surfaces of silicate layers have been modified.[5−10] It has been reported that there are three types of dispersion of layered silicates in the polymer matrix: phase separated conventional composite, intercalated nanocomposite, and exfoliated nanocomposite. In enhancing the physical property of nanocomposites, the latter two cases are known to be especially desirable.[11−13]

While the increased entropy provides the driving force for the physical adsorption process, the direct adsorption of uncharged polymers onto a clay surface seems unfavorable due to small enthalpy change of this process. Therefore, the specific interactions driven by, for example, hydrogen bonding and/or dipole−dipole interaction, play a significant role for enhancing both the homogeneous dispersion of clay particles and blend miscibility between components. Organically modified clay surface exploits either ionic association or covalent bonding with organic compounds which enhances the interaction between the polymer matrix and layered silicates.

Much effort has been focused on the development of new polymer-clay nanocomposites such as the high performance ablative materials,[14] electrorheologically sensitive particles,[15−17] stable electrooptical devices,[18] corrosion protection materials,[19] or conducting nanocomposite materials,[20−22] whereas the phase behavior and the specific interaction between the polymer matrix and clay has not been intensively studied. Since

* To whom orrespondence should be addressed. Tel.: + 82-32-860-7486. Fax: + 82-32-865-5178. E-mail addresses: hjchoi@inha.ac.kr (H. J. Choi) and ichin@inha.ac.kr (I. Chin).

(1) Alexandre, M.; Dubois, P. *Mater. Sci. Eng.* **2000**, *R28*, 1.
(2) LeBaron, P. C.; Wang, Z.; Pinnavaia, T. J. *Appl. Clay Sci.* **1999**, *15*, 11.
(3) Hoffman, B.; Dietrich, C.; Thomann, R.; Friedrich, C.; Mülhaupt, R. *Macromol. Rapid Commun.* **2000**, *21*, 57.
(4) Choi, H. J.; Vinay, S. J.; Jhon, M. S. *Polymer* **1999**, *40*, 2869.
(5) Gianellis, E. P. ***Adv****. Mater.* **1996**, *8*, 29.
(6) Vaia, R. A.; Jandt, E. J.; Gianellis, E. P. *Chem. Mater.* **1996**, *8*, 2628.
(7) Akelah, A.; Salahuddin, A.; Hiltner, A.; Baer, E.; Moet, A. *Nanostruct. Mater.* **1994**, *4*, 965.
(8) Hyun, Y. H.; Lim, S. T.; Choi, H. J.; Jhon, M. S. *Macromolecules* **2001**, *34*, 8084.
(9) Krishnamoorti, R.; Vaia, R. A.; Gianellis, E. P. *Chem. Mater.* **1996**, *8*, 1728.
(10) Vaia, R. A.; Ishii, H.; Gianellis, E. P. *Chem. Mater.* **1993**, *5*, 1694.
(11) Gianellis, E. P. *Appl. Organomet. Chem.* **1998**, *12*, 675.
(12) Chin, I.; Thurn-Albrecht, T.; Kim, H. C.; Russel, T. P.; Wang, J. *Polymer* **2001**, *42*, 5947.
(13) Kim, T. H.; Jang, L. W.; Lee, D. C.; Choi, H. J.; Jhon, M. S. *Macromol. Rapid Commun.* **2002**, *23*, 191.
(14) Vaia, R. A.; Price, G.; Ruth, P. N.; Nguyen, H. T.; Lichtenhan, J. *Appl. Clay Sci.* **1999**, *15*, 67.

10.1021/cm010498j CCC: $22.00
Published on Web 04/06/2002

the physical properties of polymer-based nanocomposites depend on the homogeneity of the dispersion and miscibility of clay particles in the polymer matrix, it is worth evaluating the strength of interaction between the polymer matrix and clay particles in nanocomposites to predict the material properties and to obtain optimal performance. Vaia and Giannelis[23] estimated the interaction between polymers and organically modified clays using a lattice model and provided a guideline for the experimental investigation. Balazs et al.[24] also investigated the phase behavior of a binary polymer/clay mixture based on their theoretical framework and predicted the phase diagram to accommodate various characteristics of the polymer and clay surface.

In the present study, we report the dispersion of a few percent of organically modified layered silicates in a miscible polymer blend and the specific interactions of binary components in the nanocomposites. As a typical example, the blend of poly(ethylene oxide) (PEO) and poly(methyl methacrylate) (PMMA) is used as the polymer matrix. Our preliminary results on the PEO/PMMA blend showed a single glass transition temperature (T_g) at all PEO concentrations and the decrease in the crystallinity of PEO with an increase in the amount of PMMA, confirming the miscibility between PEO and PMMA.[25]

The interaction between two chemical species in a nanocomposite can be described by the thermodynamic interaction energy density, B, based on the classical Flory−Huggins theory.[26] Differential scanning calorimetry (DSC) is used to determine the B values of the binary PEO/OMMT mixture and the PEO/PMMA/OMMT nanocomposite system, by combining the melting point depression and the binary interaction model, originally proposed to evaluate the specific interaction between two chemical species. Note that the B value measured between PEO and PMMA has been reported to be −0.40 cal/cm^3 by Jo et al.[25] X-ray diffraction (XRD) and mechanical testing of the polymer-clay nanocomposites are also used to provide additional information on the interaction between polymer and clay particles. By using a binary PEO/PMMA blend as the matrix, we attempted to quantify the association of OMMT with PEO and with PMMA in the nanocomposite system.

Experimental Section

Materials. PEO ($\bar{M}_w = 1 \times 10^5$) and PMMA ($\bar{M}_w = 1 \times 10^5$) were purchased from Aldrich Chemical Co. Organophilic montmorillonite (OMMT, Cloisite 25A) was obtained from Southern Clay Products and used without further treatment. The surface of the natural form of mica-type montmorillonites contains hydrated Na^+ (or K^+) ion, which is substituted by the organophilic $(CH_3)_2HTN(C_8H_{17})^+$ group [where HT denotes hydrogenated tallow (∼65 wt % of $C_{18}H_{35}-$ group, ∼30 wt % of $C_{16}H_{33}-$ group, ∼5 wt % $C_{14}H_{29}-$ group)] in OMMT. OMMT was dried under vacuum at 100 °C prior to removal of water. Since the performance of the polymer/clay nanocomposites is greatly dependent upon the dispersion of clay during mixing, OMMT was dissolved in dichloromethane (DCM) and sonicated for 60 min using an ultrasonic generator (Kyung-Il Ultrasonic Co., Korea) consisting of a magneto probe-type vibrator operated at a nominal frequency of 28 kHz, equipped with a temperature controller.[27]

Blend Preparation. The ternary mixture of PEO, PMMA, and OMMT in the form of intercalated polymer blend/clay nanocomposites was prepared by a solvent casting method using DCM (Oriental Chem. Ind., Korea) as the cosolvent.[28] PEO and PMMA were dissolved in DCM at room temperature and stirred for 48 h for complete mixing. OMMT was then added to the PEO/PMMA/DCM solution and stirred for additional 48 h at room temperature and transferred into a glass Petri dish. The nanocomposite film was dried further in a vacuum oven at room temperature. The binary mixtures of both PEO/OMMT and PMMA/OMMT in the intercalated nanocomposite forms were separately prepared by the same procedure. Preliminary XRD analyses of the PMMA/OMMT and the PEO/OMMT nanocomposites showed that the optimum clay content for intercalation was around 5 wt % in both polymer matrixes.

Differential Scanning Calorimetry. The measurement was carried out in a Perkin-Elmer differential scanning calorimeter 7, equipped with a mechanical refrigeration accessory. Dry nitrogen gas was allowed to flow through the DSC cell at a rate of 20 mL min^{-1}. DSC was calibrated using indium and sapphire as standards. In addition, the instrument was equipped with a drybox assembly, necessary to avoid signal instability due to drafts or changes in the room temperature. Low-pressure dry nitrogen gas was kept flowing at constant rate through the drybox to prevent condensation of the atmospheric moisture.

Prior to measurement, the samples were heated to 140 °C to remove the thermal history acquired during the sample preparation. For T_g measurement, specimens were quenched from 140 to −60 °C and then heated to 140 °C with a scanning rate of 20 °C min^{-1}. For the measurement of the equilibrium melting temperature (T_m^o), the sample was heated to 90 °C, maintained for 5 min to ensure complete melting of PEO crystals, quenched to the crystallization temperature T_c, kept at T_c for at least 30 min, and then heated at a heating rate of 20 °C/min.

X-ray Diffraction. The X-ray measurements were carried out in a Philips PW1847 X-ray diffractometer, performed using reflection geometry and Cu Kα radiation (wavelength $\lambda = 0.154$ nm) operated at 40 kV and 100 mA. Data were collected within the range of scattering angles (2θ) of 1−10°. The films were used without further treatment.

Transmission Electron Microscopy. TEM photographs were obtained with a JEM 2000 EX-IIU(JEOL, Tokyo, Japan) electron microscope operated at an accelerated voltage of 100 kV. All of the ultrathin sections (less than 3 μm) were microtomed using Super NOVA 655001 (R. J. Swiss) with a diamond knife and then subjected to TEM observation without staining.

Mechanical Testing. The as-prepared films of the PEO/PMMA/OMMT nanocomposite and the PEO/PMMA blend were subjected in uniaxial elongation at room temperature. All experiments were carried out with a UTM, Hounsfield test

(15) Kim, J. W.; Kim, S. G.; Choi, H. J.; Jhon, M. S. *Macromol. Rapid Commun.* **1999**, *20*, 450.
(16) Kim, J. W.; Noh, M. H.; Choi, H. J.; Lee, D. C.; Jhon, M. S. *Polymer* **2000**, *41*, 1229.
(17) Park, J. H.; Lim, Y. T.; Park, O. O. *Macromol. Rapid Commun.* **2001**, *22*, 616.
(18) Kawasumi, M.; Hasegawa, N.; Usuki, A.; Okada, A. *Appl. Clay Sci.* **1999**, *15*, 93.
(19) Yeh, J. M.; Liou, S. J.; Lin, C. Y.; Cheng, C. Y.; Chang Y. W.; Lee, K. R. *Chem. Mater.* **2002**, *14*, 154.
(20) Kim, B. H.; Jung, J. H.; Kim, J. W.; Choi, H. J.; Joo, J. *Synth. Met.* **2001**, *117*, 115.
(21) Lee, D.; Lee, S. H.; Char, K.; Kim, J. *Macromol. Rapid Commun.* **2000**, *21*, 1136.
(22) Kim, B. H.; Jung, J. H.; Hong, S. H.; Joo, J.; Epstein, A. J.; Mizoguchi, K.; Kim, J. W.; Choi, H. J. *Macromolecules* **2002**, *35*, 1419.
(23) Vaia, R. A.; Giannelis, E. P. *Macromolecules* **1997**, *30*, 7990.
(24) Balazs, A. C.; Singh, C.; Ginzburg, V. V. *Macromolecules* **2000**, *33*, 1089.
(25) Jo, W. H.; Kwon, Y. K.; Kwon, I. H. *Macromolecules* **1991**, *24*, 4708.
(26) Riedl, B.; Prudhomme, R. E. *Polym. Eng. Sci.* **1985**, *24*, 1291.
(27) Kim, C. A.; Choi, H. J.; Kim, C. B.; Jhon, M. S. *Macromol. Rapid Commun.* **1998**, *19*, 419.
(28) Choi, H. J.; Kim, S. G.; Hyun, Y. H.; Jhon, M. S. *Macromol. Rapid Commun.* **2001**, *22*, 320.

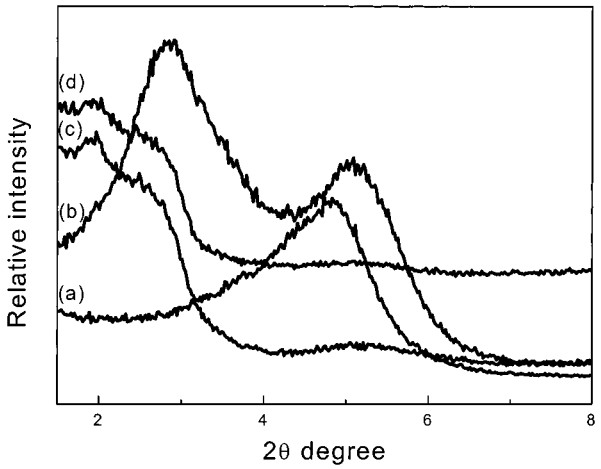

Figure 1. X-ray diffraction profile: (a) OMMT, (b) PEO/OMMT, (c) PMMA/OMMT, and (d) PEO/PMMA/OMMT.

Table 1. Observed *d*-Spacing Data for OMMT and Its Mixture with PEO and PMMA

sample	composition (wt %)	*d* (Å)
OMMT	-	17.3
PEO/OMMT	95/5	32.7
PMMA/OMMT	95/5	35.3
PEO/PMMA/OMMT	47.5/47.5 5	34.0

equipment and the typical sample dimension was 10 mm (wide) × 50 mm (length) × 1 mm (thick).

Results and Discussion

X-ray Diffraction. Figure 1a−d shows a series of the X-ray diffractograms of OMMT, PEO/OMMT, PMMA/OMMT, and PEO/PMMA/OMMT. The amount of OMMT in the mixtures was fixed at 5 wt % and, in Figure 1d, the ratio between PEO and PMMA was 50:50 by weight. X-ray intensities shown in Figure 1b−d were multiplied by a factor of 10^2 to avoid overlapping between data. The *d*-spacings in Figure 1a−d were summarized in Table 1.

In Figure 1a, a broad peak was observed at (2θ) ∼ 4.9° (the corresponding *d*-spacing ∼ 18 Å) without additional higher order peaks in the small angle region. The peak was due to a smectic-like layer ordering of OMMT at room temperature. It is likely that the peak broadness was caused by the structural imperfection of layer ordering of OMMT after modification by the $(CH_3)_2HTN(C_8H_{17})^+$ group on the surfaces. Figure 1b showed the *Bragg* peaks at (2θ) ∼ 2.7° and 5.1°. The most intense peak at (2θ) ∼ 2.7° corresponded to the *d*-spacing of 32.7 Å, which arose from the intercalated layer ordering in the mixture of PEO and OMMT. As compared with the layer thickness of OMMT, it was expanded by almost 80% in length due to intercalation. The peak observed at (2θ) ∼ 5.1° (the corresponding *d*-spacing of 17.3 Å) was either the higher order peak of the main peak at (2θ) ∼ 2.7° or one from the unintercalated OMMT layers. Since the peak at (2θ) ∼ 5.1° appeared at an angle slightly lower than expected and at an angle very close to the one for the bulk OMMT, it was more likely due to the unintercalated OMMT layers.

In Figure 1c we found broad peaks located at (2θ) ∼ 2.5° and 5.2°, also confirming the intercalation of OMMT in PMMA. The corresponding *d*-spacings were 35.3 and 17.0 Å, respectively. The complete profile of the peak at (2θ) ∼ 2.5° was not available in our wide-angle X-ray diffractometer because of the broadness of the peak. The fact that the layer thickness of the nanocomposite PMMA/OMMT was larger than that of PEO/OMMT indicates a better association or interaction between OMMT and PMMA. The broadness of the peak can be explained by the tendency of exfoliation of OMMT in the PMMA/OMMT mixture due to association.[29] The fact that the second most intense peak at ∼ 6.1° showed up as expected suggested that it might arise due to the higher order diffraction of the main peak. The possibility of the removal of the $(CH_3)_2HTN(C_8H_{17})^+$ group from the surface of OMMT during the intercalation process could be ignored because the peak at (2θ) ∼ 6.1° was not reproducible in the PEO/OMMT mixtures which were prepared by the same procedure. These results reveal that the association between PMMA and OMMT is rather substantial.

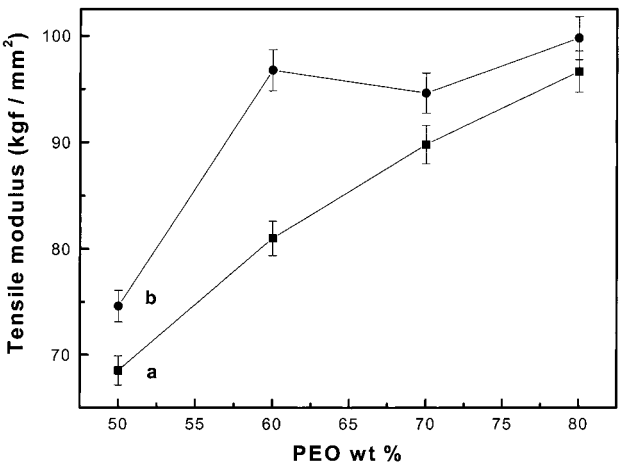

Figure 2. Tensile modulus of (a) PEO/PMMA blends and (b) PEO/PMMA/OMMT.

Figure 1d shows the X-ray diffractogram of a polymer blend/clay nanocomposite of a ternary mixture of PMMA/OMMT/PEO with a composition of 47.5/47.5/5 by weight. A broad peak was found at (2θ) ∼ 2.6°, confirming the intercalation of the polymer blend matrix within OMMT. The corresponding *d*-spacing was estimated as approximately 34 Å, which was similar to those measured for the binary mixtures of PEO/OMMT and PMMA/OMMT. Whether OMMT has the better affinity with PMMA cannot be determined by using X-ray data of the ternary mixture.

Mechanical Properties. Figures 2 and 3 show the tensile modulus and elongation at break of the PEO/PMMA/OMMT nanocomposite as a function of the PEO loading. These samples contain OMMT 5% of OMMT by weight. Data of the PEO/PMMA binary blends were also shown for comparison. As shown in both figures, the mechanical properties of nanocomposites were improved due to the intercalation of OMMT with the polymer matrix. The fact that elongation at break of nanocomposite samples was higher than that of the polymer matrix especially indicates the homogeneous dispersion of OMMT in the polymer matrix. The tensile modulus of the nanocomposites was increased with an increase in the amount of PEO. The enhancement of the

(29) Chen, G.; Chen, X.; Lin, Z.; Ye, W.; Yao, K. *J. Mater. Sci. Lett.* **1999**, *18*, 1761.

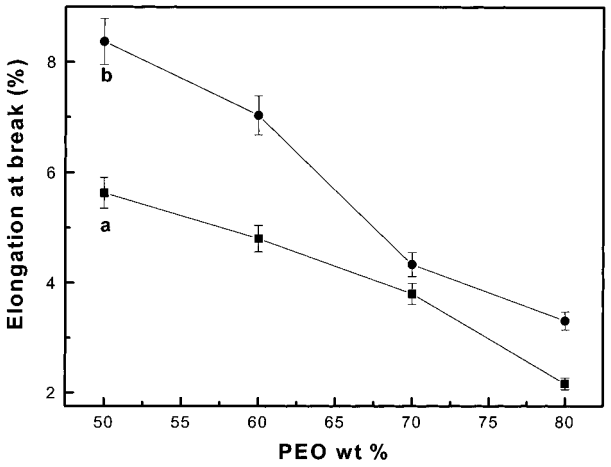

Figure 3. Elongation at break of (a) PEO/PMMA and (b) PEO/PMMA/OMMT.

modulus is reasonably attributed to the high resistance exerted by the clay against the plastic deformation, together with the effect of stretching of the oriented backbone bonds of the polymer chains in the gallery.[30,31]

Melting Point Depression and Interaction Parameter Determination. Our X-ray data for the binary PEO/OMMT and PMMA/OMMT nanocomposites provide information on the interaction between the polymer matrix and the surface of silicate layers in the mixture. Figure 1a,b shows that the layer thickness for the PMMA/OMMT nanocomposite is greater than that for the PEO/OMMT mixture, suggesting that the PMMA molecules have better affinity with the hydrophobic surfaces of OMMT than hydrophilic PEO. In addition, the broadness of the peak for the PMMA/OMMT system, indicative of a tendency of being exfoliated, also indicates the better association of OMMT with PMMA. For the PEO/OMMT mixture, the intensity of the peak located on the shoulder of the main intense peak at (2θ) $\sim$ 5.1°, appeared due to the layer ordering of the unintercalated OMMT, was almost a half of one of the main intense peak at (2θ) $\sim$ 2.7°, indicating that approximately one-third of the added OMMT was unintercalated in the mixture. The existence of the second peak in the PEO/OMMT nanocomposites suggests that the layered phase of OMMT in the PEO/OMMT mixture exhibits a biphasic behavior, consisting of the intercalated and the unintercalated OMMT layers.

The evaluation of the specific interaction between the polymer matrix and the silicate layers can be made by combining the melting point depression and the binary interaction model for heat of mixing. Our preliminary DSC data showed that the melting temperature and the heat of fusion of the PEO/OMMT mixture were decreased with the increase of the OMMT content, showing that the PEO and OMMT are miscible in a molecular level. The relation between the melting point depression and the interaction energy parameter in the mixture can be described by the following equation:[31]

$$T_m^{\circ} - T_{mix}^{\circ} = -B \frac{V_{iu}}{\Delta H_{iu}} T_m^{\circ} (1 - \phi_i)^2 \qquad (1)$$

(30) Lee, D. C.; Jang, L. W. *J. Appl. Polym. Sci.* **1996**, *61*, 1117.
(31) Nishi, T.; Wang, T. T. *Macromolecules* **1975**, *8*, 909.

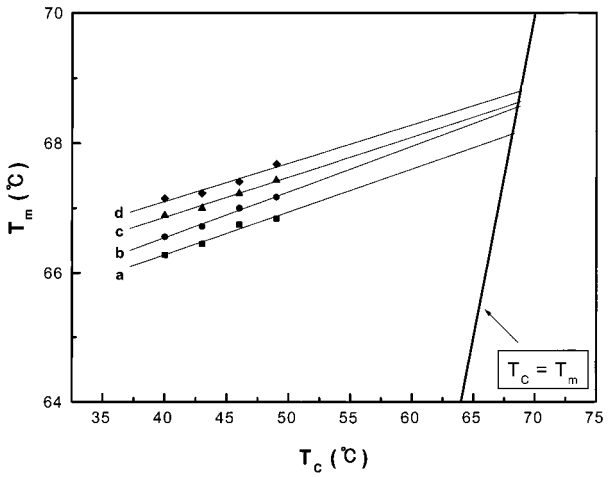

Figure 4. Hoffman−Weeks plot for the PEO/OMMT mixtures: (a) 2 wt % OMMT, (b) 5 wt % OMMT, (c) 10 wt % OMMT, and (d) 15 wt % OMMT.

Table 2. Measured Equilibrium Melting Temperatures for the PEO/OMMT Blends

composition (wt %)	T_{mix}° (°C)
100/0	73.0
98/2	68.7
95/5	68.5
90/10	68.4

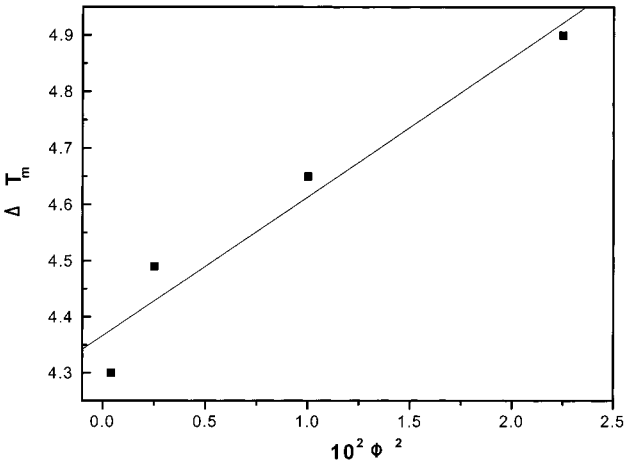

Figure 5. Plot of the equilibrium melting point of PEO in the PEO/OMMT binary mixture.

where T_m° and T_{mix}° are the equilibrium melting points of PEO and mixtures, respectively, $\Delta H_{iu} / V_{iu}$ is the heat of fusion of PEO per unit volume, ϕ_i is the volume fraction of PEO, and B is the interaction energy density between two components. The overall interaction energy density B can be obtained from the slope of the plot of $T_m^{\circ} - T_{mix}^{\circ}$ vs $(1 - \phi_i)^2$.

The equilibrium melting temperatures of pure PEO and the PEO/OMMT nanocomposites were obtained by using Hoffman−Weeks plots (Figure 4) and are listed in Table 2. Figure 5 shows the melting point depression of PEO in the PEO/OMMT nanocomposites as a function of the PEO content. According to eq 1, the B value for the PEO/OMMT mixture was determined from the slope of the straight line of Figure 4. When the values of 41.4 cm^3/mol and 20232 cal/mol were used for V_{iu} and ΔH_{iu}, respectively, in eq 1, B was estimated to be −0.35 cal/cm^3, suggesting that the PEO/OMMT mixture was miscible. The heat of mixing, ΔH_{mix}, of a

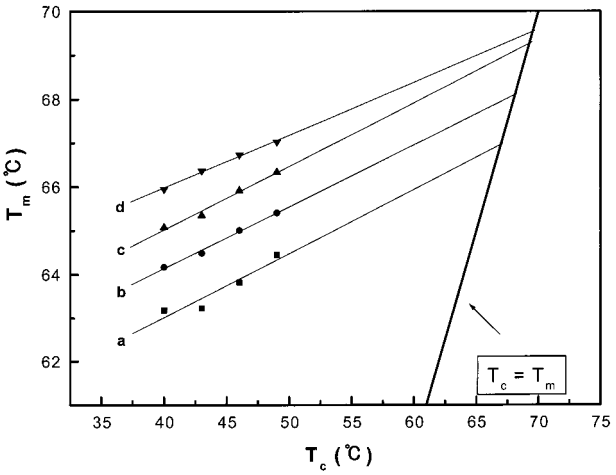

Figure 6. Hoffman−Weeks plot for the PEO/PMMA/OMMT mixtures: (a) 47.5/47.5/5, (b) 57/38/5, (c) 66.5/28.5/5, and (d) 76/19/5.

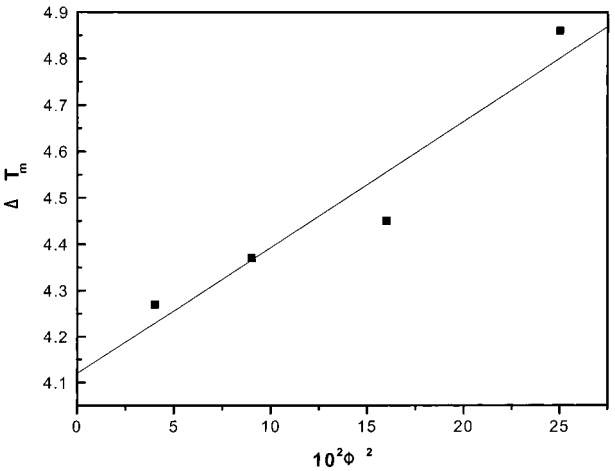

Figure 7. Plot of the equilibrium melting point of PEO in the PEO/PMMA/OMMT ternary mixture.

Table 3. Measured Equilibrium Melting Temperature for the PEO/PMMA/OMMT Mixtures

composition (wt %)	T_{mix}^o (°C)
76/19/5	68.7
66.5/28.5/5	68.6
57/38/5	68.6
47.5/47.5/5	68.1

multicomponent system can be described in terms of the binary interaction parameters by

$$\Delta H_{mix} = V \sum_i \sum_{i \neq j} B_{ij} \phi_i \phi_j \qquad (2)$$

where V is the system volume, B_{ij} is the interaction energy density, and ϕ_i and ϕ_j are the volume fraction of component i and j in the mixture, respectively. In case of binary mixtures, $\Delta H_{mix} = 0$ becomes the criterion for predicting a boundary between the single-phase and the multiphase behavior.

In a ternary mixture of polymer A, clay B, polymer C, let polymer A be comprised of monomer 1 and clay B and polymer C be comprised of 2 and 3, respectively. In the mixture of A, B, and C, the volume fractions occupied by the various basic units 1, 2, and 3, respectively, are f1, f2, and f3. For a ternary mixture of A, B, and C, the heat of mixing is given by eq 3:

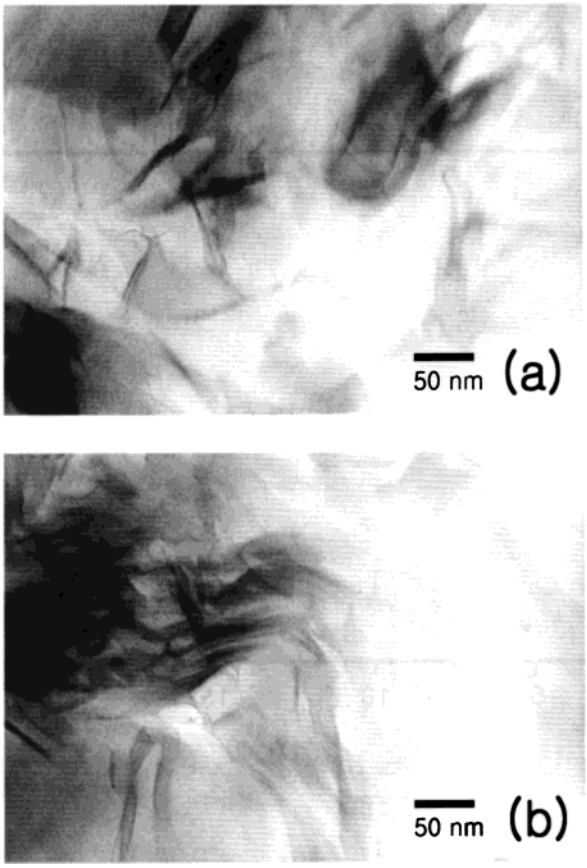

Figure 8. TEM images of (a) PEO/OMMT and (b) PEO/PMMA/OMMT ternary mixture.

$$\Delta H_{mix} = V \sum_{i \neq j}^{3} B_{ij} \phi_i \phi_j \qquad (3)$$

Accordingly, the partial molar enthalpy of component 3, $\Delta \bar{H}_3$, was derived as eq 4 [where $\psi_i = \phi_i/(1 - \phi_3)$]:

$$\Delta \bar{H}_3 = V_3(B_{12}\psi_1\psi_2 + B_{23}\psi_2\psi_3 + B_{13}\psi_1\psi_3)(1 - \phi_3)^2 \qquad (4)$$

where V_3 is the molar volume of component 3 and ϕ_i is the volume fraction of component i in the mixture. Consequently, overall interaction energy density B in the blend is related with segmental interaction energy densities B_{ij}'s by the following relation:

$$B = B_{12}\psi_1\psi_2 + B_{23}\psi_2\psi_3 + B_{13}\psi_1\psi_3 \qquad (5)$$

Equation 1 suggests that the parameter B for a ternary blend can be evaluated from the slope of T_m^o versus the square of the $(1 - \phi_i)$ in exactly the same way as for a binary blend.

To apply eq 5 to the present ternary blends, we denoted MMA by 1, OMMT by 2, and ethylene oxide (EO) by 3. There are three segmental interaction energy parameters in the present ternary blends. Among them, B_{13} of −0.40 cal/cm^3 was determined in the previous study.[25] The value of B_{23}, corresponding to the interaction between PEO and OMMT, was directly obtained from the melting point depression of PEO in the PEO/OMMT mixture. The value was −0.35 cal/cm^3, as

evaluated in the previous section. The overall interaction parameter B has been evaluated from the equilibrium melting point depression at a given ψ_i, which corresponds to the PMMA/OMMT/PEO ratio. The equilibrium melting points were determined from the Hoffman−Weeks plots, as shown in Figure 6. Table 3 summarizes the equilibrium melting temperature of PEO in the ternary mixtures containing 1:1 PEO/PMMA.

Figure 7 shows plots of the equilibrium melting point depression of PEO versus the square of the volume fraction of the remaining part in the ternary mixture. The data can be fitted in a straight line and its slope determines the overall interaction parameter B as −1.30 cal/cm^3. Upon substitution of overall interaction parameter and the corresponding values into eq 5, the unknown parameter B_{12} was calculated to be −13.87 cal/cm^3. The estimated interaction parameters of pairs suggested that the interaction between PMMA and OMMT was the most favorable.

Figure 8 exhibits the TEM images of (a) PEO/OMMT and (b) PMMA/PEO/OMMT, respectively. Dark bundles of OMMT which are poorly dispersed and intercalated are shown in Figure 8a. On the other hand, Figure 8b represents a well-ordered layer structure of OMMT, which clearly confirms the entries of PEO/PMMA blend in the layer of OMMT, indicating better association of PMMA matrixes on the surfaces of OMMT.

Conclusions

The Flory−Huggins interaction parameters B's between polymers and silicate layers in a PEO/PMMA/OMMT mixture were determined. The values were −13.87 and −0.35 cal/cm^3 for $B_{PMMA/OMMT}$ and, $B_{PEO/OMMT}$ respectively, suggesting that PMMA and OMMT are highly miscible. The larger layer thickness and broadness of the peak for the PMMA/OMMT mixture also indicate a better intercalation or association of PMMA matrix on the surfaces of OMMT. The relatively weak association between PEO and OMMT may be due the hydrophobic modification of the surface of clay. The modification of the surface characteristics of the platelet type silicate enhances the mechanical properties of the nanocomposites.

Acknowledgment. Authors acknowledge the financial support from Inha university through special funding program of 2000. H. J. C. appreciates research grants from the Korea Science and Engineering Foundation (KOSEF) through the Applied Rheology Center (ARC), an official KOSEF-created engineering research center (ERC) at Korea University, Korea.

CM010498J